RESEARCH ARTICLE

Assessment of 3D Printability of Sweetened Heat Desiccated Concentrated Milk-based Formulations for Preparation of Dairy Sweetmeat (*Burfi*)

Deepak Vats¹, Kaushik Khamrui¹ (⋈), Writhdhama Prasad¹, Jatindra K Sahu² and Satheeshkanth SSM²

Received: 19 January 2025 / Accepted: 21 March 2025 / Published online: 23 August 2025 © Indian Dairy Association (India) 2025

Abstract: This study was aimed to develop formulations for 3D printing of *burfi*, with detailed rheological characterization and printability. Milk-concentrate and sugar-based formulations possessed poor printability hence rheology modifiers *viz.*, xanthan gum and corn flour were added. Apparent viscosity, yield stress and storage modulus were critical for 3D printing. Xanthan gum imparted superior print quality as compared to corn flour added formulations due to the pronounced shear thinning behaviour. Formulation prepared using milk concentrated to 45% TS, added with 30% sugar and 0.5% xanthan gum exhibited highest dimension accuracy factor (97.01%) and found to be best suited for 3D printing.

Key words 3D printing, Rheology, Dairy Technology, Burfi

Introduction

3D printing (3DP) is an emerging manufacturing technology that employs layer-by-layer fabrication of an object having a complex structure from a pre-determined shape. It has been successfully acknowledged in dairy and food industries in recent times to fabricate food constructs with novel texture, structure, function and sensory qualities (Sharma et al. 2024). Concentrated milk-based sweets are very popular in the Indian subcontinent. 3D food printing is considered as a potential technology to achieve food personalization, automation, reduce wastage, standardize

modifiers (RM) (Lee et al. 2020).

Xanthan gum and corn flour are one of the most commonly used additives added in bio-inks to make them easily extrudable and to improve the self-supporting structure of the 3D printed constructs after printing. Xanthan gum-based food inks exhibit strong shear-thinning and shear recoverability characteristics whereas corn flour act as a gelling agent in food inks (Liu et al. 2018). By altering their rheological parameters, these compounds improve the printability and shape fidelity of the food inks. The present study was aimed to evaluate the printability of heat desiccated sweetened milk concentrated based formulations in combination with two RM *viz.*, xanthan gum and corn flour, to fabricate complex structures of dairy sweetmeat *i.e.*, *burfi*. Specifically, the changes in rheological and textural attributes of

the formulations with different concentration levels milk concentrate and sugar were assessed, and their combined impact on the printing accuracy and structural stability of the 3D printed

texture, maintain consistent quality and to reduce drudgery

involved in conventional manufacturing processes (Choudhury

et al. 2024). In recent times, a lot of information is available on

rheological characterization and 3D printing of chocolate,

confectionery, cereal, meat and vegetables-based formulations

(food inks) (Suzuki et al. 2019). However, concerning 3D printing

of dairy products, most of the work has been limited to printing

of milk powder-based formulations and processed cheese. There

still remains an urgent need to study the 3D printing of traditional

Indian dairy products to establish correlation between rheological

behavior of the formulations (food inks) with their 3D printability.

3D printing of food inks depends highly upon their rheological attributes *viz.*, flow behaviour, yield stress, shear recoverability,

thermo-responsive behaviour etc. Food inks must be flowable enough to extrude easily through the printing nozzle vis-à-vis

having enough yield stress and mechanical strength to support itself after extrusion through 3D printer. Heat desiccated milk

solids-based formulations lacked structural integrity after

extrusion through 3D printer due to irrecoverable damage to their

internal microstructure and therefore, to 3D print heat desiccated

milk solids-based formulations, their rheological characteristics

needed to be improved with addition of additives called rheology

¹Dairy Technology Division, ICAR-National Dairy Research Institute, Karnal – 132 001, Haryana, India

²Centre for Rural Development and Technology, Indian Institute of Technology, New Delhi – 110 016, India.

(⊠)Corresponding author, Phone: 0184 2259242, Fax: 0184 2250042, E mail: kkhamrui@gmail.com

constructs was evaluated.

Materials and Methods

Raw materials and ingredients

Full cream milk (6% Fat, 9% SNF) procured from local market of Karnal, Haryana, India was used to make open pan heat desiccated milk concentrate (MC). Xanthan gum powder was procured from M/s Sigma Aldrich Chemicals Private Limited, Delhi. Powdered cane sugar (sucrose) and corn flour of reputed brand were procured from local market of Karnal, Haryana, India.

Preparation of different formulations (food inks) by adding rheology modifiers

MC was prepared using open heat desiccation to 42-53% TS content. After determining the actual solid content, the exact TS level was adjusted using warm potable water (50ÚC). While maintaining the temperature at 60-62ÚC, powdered sugar and the RMs *viz.*, xanthan gum or corn flour were added to the standardized MC. Heating was continued with continuous mixing and kneading to obtain a semi-solid mass. The mix was then cooled and homogenized using Ultra-turrax homogenizer at 5000 RPM for 3 min at 50ÚC to produce uniform mass. Finally, the temperature was again raised to 80ÚC/10 sec to ensure microbiological safety, followed by hot packaging in PET bottles. Formulations were prepared according to the experimental design presented in Table 1 using MC, powdered sugar and RM.

3D printing process

An extrusion-based screw-driven 3D printer (Hyrel3D Engine SR) was used to assess the printability of studied formulations. A rectangular cuboid model was designed with three cm each in length, breadth and one cm height to imitate the shape of *burfi* and printed with constant printer settings of nozzle diameter: 1.2 mm, printing speed: 15 mm/s, layer height: 0.96 mm (80% of nozzle diameter), printing pattern: recti-linear and in-fill percentage:100%. The 3D printing process were carried out at $30\pm1\text{\'UC}$.

Rheological analysis of prepared formulations

Rheological characteristics were analyzed using a dynamic rotational and oscillatory rheometer (MCR-52, Anton Paar, Austria). Measurements were conducted using parallel plate geometry with a diameter of 50 mm (PP-50) with a gap of 0.5 mm. The rheological characteristics of the formulations were carried out at $30\pm1\text{UC}$.

Shear viscosity test

The shear-viscosity tests were conducted in a ramp linear mode by increasing the shear rate from 0.01 to 100 s "1. The experimental values of the shear stress and strain were fitted to the Power law $(\tau = k\gamma^n)$ and the Bingham model $(\tau = \tau_0 + k\gamma^n)$, where τ is the shear

stress (Pa), γ is the shear rate (s"1), k is the consistency index (Pas"), n is the flow behavior index and τ_o is the yield stress (Pa). The goodness of fit of the models was evaluated by determining the coefficient of determination (R²).

Amplitude and frequency test

The oscillatory tests were performed at 6.28 rad s"1 with strain sweeps from 0.01-100% to identify linear viscoelastic region (LVR). Yield stress (τ_0), frequency sweep, storage (G') and loss (G") moduli were determined according to Joshi et al. (2021).

Rotational recoverability test

The shear recoverability of formulations and recovery index was determined by applying a low shear rate $1 \, \text{s}^{"1}$ for $180 \, \text{s}$, followed by a high shear rate $100 \, \text{s}^{"1}$ for $180 \, \text{s}$ and finally, a low shear rate $1 \, \text{s}^{"1}$ for $300 \, \text{s}$.

Evaluation of printing quality

Four tests were performed to evaluate the printing quality of 3D printed constructs as discussed below.

Dimensional Accuracy Factor (DAF)

DAF in terms of length, width and height of the printed constructs was determined by comparing the dimensions of 3D model design and printed constructs. Dimensions of 3D constructs using the following formula.

DAF =
$$[1 - \frac{\text{Deviation in linear dimension from the target}}{\text{Linear dimension of the target}}] \times 100$$

Shape Inconsistency Factor (SIF)

To calculate the SIF, the area of each side (six) was measured using image analysis (ImageJ software version 1.8.0). Each measured area was divided by its theoretical value and the average of the standard deviation of these values multiplied by 100 was defined as SIF (Lipton et al. 2015).

Assessment of dimensional shape stability

Shape stability of 3D printed constructs over time is an important parameter to judge its printing quality. It was evaluated by calculating change in area of 3D printed construct over timelapse of 10, 20, 30 and 60 minutes.

Assessment of deformation in 3D printed constructs

Deformation in 3D printed construct is the irregularity between top face and bottom face of cuboid which is evaluated using Deformation Factor (DF). The Deformation Factor is the ratio of the area of the top to the bottom faces (Gholamipour et al. 2019).

Determination of total solids content

TS content was determined using the gravimetric procedure described by Choudhury et al. 2024.

Experimental design and statistical analysis

TS content of MC milk concentrate was varied at three different levels *i.e.*, 40, 45 and 50% based on initial experiments. Sugar content was varied at three different levels 20, 25 and 30% to study the effect of sugar concentration on printability of foodinks. The rheology modifiers *viz.*, xanthan gum (XG) at 0.5% and corn flour (CF) at 5% were selected at fixed concentration. In total 18 formulations (F1 to F18) were studied for their printability (Table 1). Based upon level of TS content in MC and sugar added the combinations were coded from K40- S20 to K50 S30.

Data obtained from various experiments were subjected to analysis of variance (one way and two way) followed by Tukey's post hoc comparison test to establish the significance of differences by employing SPSS software.

Results and Discussion

Rheological characterization of the formulations

Shear thinning behaviour

Shear stress decreased drastically for all the formulations as shear rate was increased from 1-20 s⁻¹ and thereafter it was relatively constant throughout the test i.e., all the formulations exhibited shear thinning behavior which is highly desirable for 3D printing. All formulations showed yield stress that has to be overcome to get relatively constant apparent viscosity value against increasing shear rate. Shear thinning tendency is the most important behavior that food-inks must possess in order to pass through small nozzle of 3D printer (Lee et al. 2020). Decrease in values of shear stress in the range of 1-20 s⁻¹ was more prominent for formulations having xanthan gum as RM indicating their more dominant shear thinning and pseudoplastic behavior as compared to corn flour (Fig. 1). This was also confirmed by negative values of consistency index when power law model was applied. It can be seen from Table 2 that power law model was found to be best fit (R² e" 0.75) for all the formulations. Consistency index (K) indicates about the apparent viscosity of the food system and it was highest for F15 at 4.64 and lowest for F2 at 2.43. Formulations having xanthan gum as RM generally exhibited significantly (p<0.05) higher consistency index as compared to corn flour based formulations. It can also be observed that with increase in total solids of formulations values of consistency index also increased significantly (p<0.05). Gnezdilova et al. (2015) found that adding starch syrup, malt, or demineralized whey powder to the products results in the deviation of their rheological characteristics to more non-Newtonian pseudoplastic behaviour. Lee et al. (2020) also reported an increase in shear thinning behaviour and decrease in flow behaviour index from 0.86 to 0.50 of milk-powder based formulations with increase in total solid content from 10 to 75%.

Yield stress, recoverability index and phase angle of the formulations

Yield stress is a characteristic exhibited by viscoelastic foods and it is the minimum stress at which food samples start to flow. The formulations exhibited yield stress which ranged from 749 - 2880 Pa and 215.67 - 1473.33 Pa for the samples having xanthan gum and corn flour as RM, respectively (Table 3). Significant (p<0.05) increase in yield stress was observed for both xanthan gum and corn flour added formulations as the total solids content (%w/w) increased from 50.25% to 62.99%. Joshi et al. (2021)

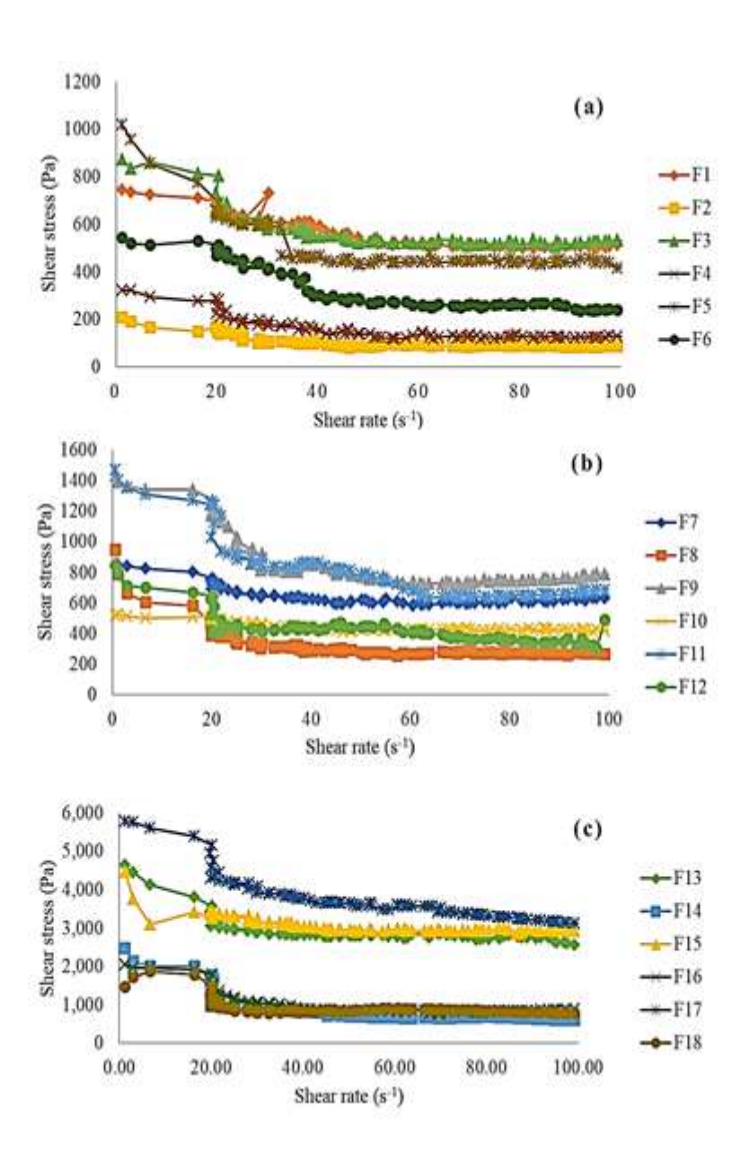


Fig 1 Shear stress vs shear rate curve for formulations (a) F1 to F6 (b) F7 to F12 (c) **F13 to F18** (F1-F18 are formulations as described in Table 1)

Table. 1: Experimental design

		0	S30	CF	F18
		30	K50_S30	XG CF	F17 F18
3	50	25	K50_S25	CF	F16
			Y	XG	F15
		20	K50_S20	CF	F14
				XG	F13
		30	K45_S30	XG CF	F12
			K45	XG	F11 F12
2	45	25	S25	XG CF	F10
		7	K40_S30 K45_S20 K45_S25	XG	F5 F6 F7 F8 F9 F10
		20	_S20	XG CF	F8
		(1	K45	XG	F7
		30	S30	XG CF	F6
			K4(XG	F5
1	01	25	S25	CF	F4
	7	(1	K40_S20 K40_S25	XG CF XG CF	F1 F2 F3 F4
		20	_S20	CF	F2
		7	K40	XG	F1
Ingredients	Milk Concentrate (MC) (T.S. % w/w)	Sugar (% w/w of MC)	Denotation	KM (CF 5 % of MC, XG 0.5 % of MC)	Denotation

Table 2: Estimated rheological parameters of formulations using power law model

MC and		u				KO	K (Pa.s)			č	2	
ugar combination										1	,	
	XG		CF		XG		CF		XG		CF.	
.40_S20	F1	$-0.44\pm0.03^{\mathrm{fB}}$	F2	$-0.26\pm0.06^{\mathrm{bcA}}$	F1	3.5 ± 0.11^{abA}	F2	2.43 ± 0.06^{fB}	F 1	0.91+0.01 ^{aA}	7 2	O 78+O OAbcdB
.40_S25	F3	$-0.16\pm0.02^{\mathrm{abcA}}$	F4	-0.27 ± 0.12^{bcA}	F3	3.04 ± 0.05^{abA}	F4	2.69±0.16 ^{eB}	F3	0.81±0.01	F.4	0.78 ± 0.04
40_S30	F5	$-0.24\pm0.02^{\text{deA}}$	F6	-0.3 ± 0.042^{bcA}	F5	3.09 ± 0.04^{abA}	F6	3.01 ± 0.04^{cdB}	F5	0.83 ± 0.05	F T EK	0.55±0.01
45_S20	F7	$-0.11\pm0.01^{\mathrm{aA}}$	F8	$-0.27\pm0.04^{\text{bcB}}$	F7	$2.98\pm0.03^{\rm bA}$	ж Ж	2 94±0 017 ^{dA}	F7	0.83±0.010	2 K	0.7240.03
45_S25	F9	$-0.23\pm0.05^{\mathrm{cdeB}}$	F10	-0.08 ± 0.02^{aA}	F9	3.27 ± 0.05^{abA}	F10	$2.77 \pm 0.06^{\text{deB}}$	F9	0.75±0.01	F10	0.50±0.01 0.72±0.01 ^{dB}
K45_S30	F11	$-0.26\pm0.02^{\mathrm{eB}}$	F12	-0.21 ± 0.01^{abA}	F11	3.33 ± 0.02^{abA}	F12	2.98±0.01 ^{dB}	F11	$0.81 \pm 0.03^{\rm bA}$	F17	0.72±0.01
$50_{-}S20$	F13	-0.12 ± 0.01^{abA}	F14	$-0.39\pm0.02^{\text{cB}}$	F13	3.67 ± 0.02^{abA}	F14	3.58 ± 0.16^{aA}	F13	$0.83+0.04^{\text{bA}}$	F14	0.76 ± 0.02
50_S25	F15	-0.09 ± 0.01^{aA}	F16	$-0.28\pm0.10^{\text{bcB}}$	F15	4.64 ± 0.78^{aA}	F16		F15	0.89±0.02ªA	F16	0.78+0.01 bcdB
K50_S30	F17	$-0.18\pm0.04^{\mathrm{bcdA}}$	F18	$-0.19\pm0.01^{\mathrm{abA}}$	F17	$3.88{\pm}0.14^{abA}$	F18		F17	0.9 ± 0.04^{aA}	F18	$0.8\pm0.013^{ m bcB}$

Values are mean ± standard error (n=3); Within rows, values with different superscripts (lowercase letters) differ significantly (p<0.05); Within columns, values with different superscripts (uppercase letters) differ significantly (p<0.05); (F1-F18 are formulations as described in Table 1)

Table 3: Yield stress, recoverability index and phase angle of the formulations

MC and		Yield Stress τ_0 (P	SS T ₀ (Pa)		Recoverability index (RI %)	index ((RI %)		Phase angle (in degrees) at 1 Hz	legrees) at 1 Hz
sugar combination XG	XG		CF		XG		CF		XG		CF	
K40 S20	F1	$749.67{\pm}10.15^{\rm h}$	F2	215.67±21.36 ¹	F1	$48.95\pm0.76^{\text{deA}}$	F2	7.25 ± 0.22^{hB}	F1	21.45 ± 0.198^{a}	F2	25.36 ± 0.379^{a}
K40_S25	F3	881.67 ± 16.07^{8}	F4	317.33 ± 15.53^{h}	F3	53.59 ± 0.89^{abA}	F4	$9\pm0.20^{\mathrm{gB}}$	F3	$20.45\pm0.036^{\mathrm{bc}}$	F4	$24.06\pm0.054^{\rm b}$
K40_S30	F5	1030.87 ± 17.32^{f}	F6	548.67±9.81g	F5	56.59 ± 1.66^{aA}	F6	$9.82\pm0.05^{ ext{fB}}$	F5	20.31 ± 0.045^{bc}	F6	23.27 ± 0.065^{c}
K45_S20	F7	1205.67 ± 8.08^{e}		$788.67\pm9.81^{\rm f}$	F7	$52.16\pm1.01^{\text{bcdA}}$	F8	13.14 ± 0.18^{dB}	F7	$20.77\pm0.075^{\rm b}$	F8	$22.47\pm0.08^{ m d}$
K45_S25	F9	1400.34 ± 17.32^{d}		924.54 ± 5.2^{e}	F9	53.16 ± 1.72^{abcA}	F10	$12.12\pm0.27^{\mathrm{eB}}$	F9	$20.23\pm0.055^{\mathrm{bc}}$	F10 2	21.75 ± 0.066^{e}
K45 S30	F11	1416.67 ± 28.87^{d}		992.12 ± 6.93^{d}	F11	$56.38\pm0.36^{\mathrm{aA}}$	F12	$17.63\pm0.36^{\text{cB}}$	F11	$19.83\pm0.618^{\circ}$	F12	$20.93{\pm}0.07^{\mathrm{f}}$
K50_S20	F13	2056.56 ± 10.39^{c}		$1096.67 \pm 11.55^{\circ}$	F13	$50.01\pm1.59^{\text{cdeA}}$	F14	$22.99\pm0.24^{\text{bB}}$	F13	$18.93\pm0.084^{ m d}$	F14	20.43 ± 0.074^{8}
K50_S25	F15	2480.54 ± 17.32^{b}	F16	1213.33±57.74 ^b	F15	$51.38{\pm}1.66^{\text{bcdA}}$	F16	25.41 ± 0.31^{aB}	F15	18.67 ± 0.051^{d}	F16	$18.91\pm0.095^{\rm h}$
$K50_{330}$	F17	2880.76 ± 17.32^{a}		1473.33 ± 23.09^{a}	F17	$46.54\pm0.74^{\rm eA}$	F18	24.96 ± 0.13^{aB}	F17	18.33 ± 0.038^{d}	F18	18.04 ± 0.04^{i}

Values are mean ± standard error (n=3); Within rows, values with different superscripts (lowercase letters) differ significantly (p<0.05); Within columns, values with different superscripts (uppercase letters) differ

significantly (p<0.05); (F1-F18 are formulations as described in Table 1)

reported that yield stress increased from 229 to 1211 Pa with increase in total solids content in heat desiccated milk solids-based formulations. Similar trends were observed by Lille et al. (2018) wherein the minimum yield stress of 61.1 Pa was required for semi skimmed milk powder-based formations of 3D constructs to retain desired shape after printing.

Recoverability i.e., ability of formulations to recover as close as possible to their original viscosity after removal of high shear rates, is quantified by determining recoverability index. Recoverability index for all heat desiccated milk solids-based formulations (F1 to F18) is reported in Table 3. Formulation F5 showed highest recoverability index (56.59%) whereas F2 showed lowest (7.25%). Xanthan gum-based formulation showed significantly higher shear recoverability index (46.54-56.58%) than corn flour-based formulations (7.24-25.41%). This could be due to quick formation of the highly ordered network of entangled and stiff molecules at lower shear stress (Zhao et al. 2020). In case of corn flour-based formulations, the native continuous casein network was interrupted by association between aggregated caseinate and flour particles (Joshi et al. 2021). Paxton et al. (2017) suggested lower recoverability index for formulations might be due to permanent structure breakdown caused by high shear rate which renders the system unable to recover to original viscosity. Also, because of diverse structure and complex rheology, soft matter systems show low shear recoverability (Stokes and Frith, 2008). Similar trends were observed by Bareen et al. (2021) for heat acid coagulated milk semi-solids based formulations when shear rate changed from 100 s"1 to 1 s"1. During 3D printing of various hydrocolloid gels, Gholamipour et al. (2019) reported recoverability index to be 48±0.89%, 57.24±0.94%, $67.6\pm0.64\%$ for gels containing xanthan gum at 2%, 4% and 8%, respectively. It was also observed that phase angle was significantly lower (p<0.05) for xanthan gum added formulations at lower TS levels. This decrease in values of phase angle is an indicator that food system is attaining more solid-like behaviour.

Viscoelastic behaviour of the formulations

Amplitude sweep and frequency sweep test of the formulations revealed viscoelastic behaviour within Linear viscoelastic region (LVR) in 0.01% region of frequency strain. Food-inks showed higher storage modulus (G') than loss modulus (G") at any point in LVR As can be observed in Fig. 2 the system maintained solid like behaviour within LVR with storage modulus (G') > loss modulus (G") *i.e.*, elastic component dominating over viscous component of the food system. Further, it was observed that G' and G" were significantly (p<0.05) higher for formulations having xanthan gum as RM as compared to formulations added with corn flour (Fig 3). Also, with increase in total solids content of formulation, the gap between G' and G" was found to be increasing with G' dominating over G indicating more solid-like consistency at higher TS level. Choudhury et al. (2024) also found that if G' > G" for food inks, then food inks will show better

resistance to deformation and their 3D constructs will be more stable

It was found that there was significant increase in structural integrity of 3D constructs with an increase in G' and G" values. For formulations containing xanthan gum as RM with lower TS content (F1, F3 and F5), the 3D constructs made therefrom were symmetrical, smooth with excellent shape retention characteristics. Better shape retention was confirmed with relatively lower change in area of 3D constructs over the time as compared to corn flourbased formulations. This might be due to better shear recoverability of xanthan gum containing samples as witnessed by their higher recoverability index (Table 3). For the 3D constructs made from formulations having higher TS content viz., F15 and F17 were very poor in terms of printability with visible breakage of printing filaments. This might be due to very high values of consistency index (K) viz., 4.64 and 3.87, respectively. Liu et al. (2018) developed 3D printed milk protein food simulant using whey protein isolate (WPI) powder and milk protein concentrate (MPC) powder-based formulations having xanthan gum (0.5%) as structuring agent. It was established that addition of WPI reduced the apparent viscosity of the food system and made it smoothly printable.

Assessment of the quality of 3D printed constructs (burfi)

Dimensional accuracy factor (DAF)

The DAF for 3D constructs printed from all 18 formulations is shown in Table 4. DAF was highest for F5 (prepared using MC containing 40% TS, 25% sugar and 0.5% xanthan gum) at 97.01% and lowest for F10 (MC standardized at 40% TS content, added with 25% sugar and 5% corn flour) at 79.88%. All formulations having xanthan gum as RM, except F17 showed significantly (p<0.05) higher DAF than formulations having corn flour as RM. It could be due to better recovery index for xanthan gum-based formulations as shown in Table 4. Joshi et al. (2021) calculated DAF for 3D printed constructs from dairy matrix in terms of height, length and breadth separately. It was reported that DAF along height, length and breadth of construct was in the range of 95.29-98.78%, 96.84-99.74%, and 59.74-90.91%, respectively. Similarly, Dick et al. (2019) calculated dimensional printing deviation for 3D printed constructs of meat by directly dividing dimensional deviation with original dimension and it ranged from -0.005%-1.42%, -0.05% -1.67%, and 1.43% - 11.04% for the length, width and height, respectively.

Shape inconsistency factor (SIF)

The SIF is measure of degree of inconsistency between different edges, lines or designs in a 3D construct *i.e.*, lower the value of SIF, better will be printing quality of 3D construct. SIF was found to be highest for F2 (MC standardized at 40% TS added with 20% sugar and 5% corn flour) at 16.11±0.78, whereas lowest for F9 (MC standardized at 45% TS added with 25% sugar and 0.5%

Table 4: Dimensional accuracy factor, Shape inconsistency factor and deformation factor of 3D printed constructs

Khoa and		Dimensional accuracy	-	factor (%)		Shape inconsistency factor	stency	factor		Deformation factor	ion fac	tor
sugar combination		XG		CF		XG		CF		XG		CF
K40 S20	F1	$92.92\pm0.47^{\mathrm{Aab}}$	F2	$81.43{\pm}0.85^{\mathrm{Babc}}$	F1	$1.55\pm0.08^{\mathrm{cdB}}$	F2	$16.11\pm0.77^{\mathrm{aA}}$	F1	$0.97 \pm 0.004^{\rm cA}$	F2	$0.92\pm0.004^{\mathrm{eB}}$
$K40_S25$	F3	$92.99\pm1.21^{\text{Aab}}$	F4	$80.90{\pm}1.52^{\mathrm{Bbc}}$	F3	$1.55{\pm}0.06^{\mathrm{dB}}$	F4	$14.02\pm0.93^{\rm bcA}$	F3	$0.98{\pm}0.004^{ m boA}$	F4	$0.93{\pm}0.006^{ m deB}$
K40 S30	F5	$97.01\pm0.55^{\mathrm{Aa}}$	F6	$83.68\pm 2.17^{\mathrm{Babc}}$	F5	$0.96\pm0.024^{ m bcB}$	F6	15.00 ± 0.76^{abA}	F5	$0.98{\pm}0.003^{\mathrm{cA}}$	F6	$0.93\pm0.006^{\mathrm{cdB}}$
K45 S20	F7	$90.02\pm2.10^{ m Abc}$	F8	$81.57{\pm}2.00^{\mathrm{Babc}}$	F7	$0.59\pm0.07^{\mathrm{aB}}$	F8	$12.59\pm0.52^{\text{cA}}$	F7	$0.99\pm0.006^{ m apA}$	F8	$0.94{\pm}0.001^{ m bcB}$
K45 S25	F9	$90\pm0.36^{ m Abc}$	F10	$79.88{\pm}1.70^{\mathrm{Bc}}$	F9	$0.29\pm0.01^{\mathrm{aB}}$	F10	$8.65{\pm}0.32^{ m dA}$	F9	$0.99\pm0.001^{\mathrm{aA}}$	F10	$0.95{\pm}0.001^{ m bcB}$
K45_S30		87.99 ± 1.69^{Ac}	_	$83.11\pm1.74^{\text{Babc}}$	F11	$0.88\pm0.02^{ m bcB}$	F12	$10.02\pm0.28^{\text{dA}}$	F11	0.99 ± 0.001^{aA}	F12	$0.95\pm0.001^{\mathrm{bcB}}$
K50 S20	F13	$90.87 \pm 0.64^{ m Abc}$	F14	$85.76\pm1.25^{\text{Bab}}$	F13	$1.05{\pm}0.06^{ m bcB}$	F14	$2.96\pm0.28^{\rm eA}$	F13	$0.99\pm0.001^{\mathrm{aA}}$	F14	$0.96\pm0.001^{\mathrm{aB}}$
K50_S25	F15		F16	$86.33\pm0.60^{\mathrm{Ba}}$	F15	$1.64\pm0.17^{ m aB}$	F16	$2.85\pm0.33^{\rm eA}$	F15	$0.99\pm0.001^{\mathrm{aA}}$	F16	$0.96\pm0.001^{\mathrm{aB}}$
K50_S30	F17	$83.23\pm1.95^{\mathrm{Bd}}$	F18	83.99±2.65 ^{Aabc}	F17 1	$1.62\pm0.30^{\mathrm{aB}}$	F18	F18 3.29±0.33 ^{eA}	F17	F17 0.99 ± 0.001^{aA}	F18	F18 0.97±0.001 ^{aB}

Values are mean ± standard error (n=3); Within rows, values with different superscripts (lowercase letters) differ significantly (p<0.05); Within columns, values with different superscripts (uppercase letters) differ significantly (p<0.05); (F1-F18 are formulations as described in Table 1)

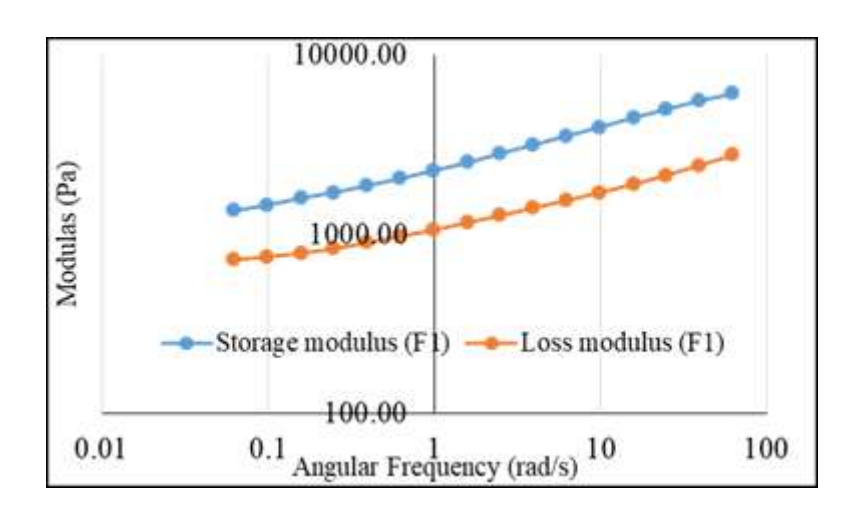
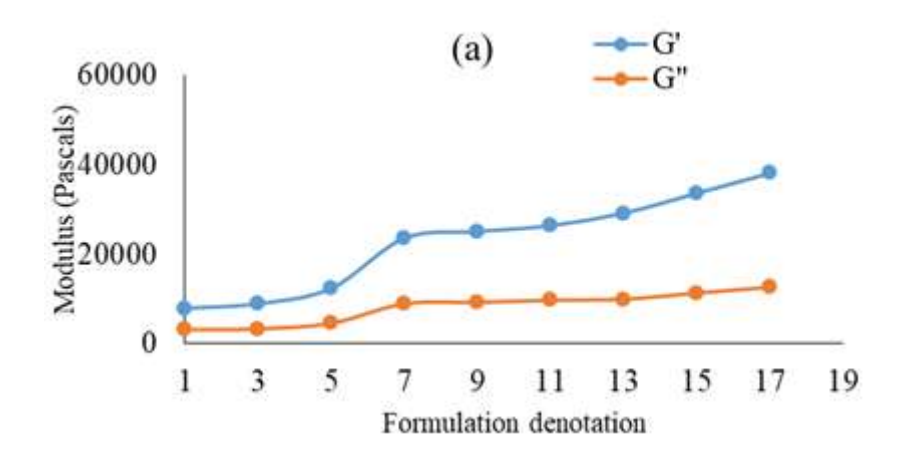


Fig. 2 Typical G' and G" increase in LVR region of a formulation



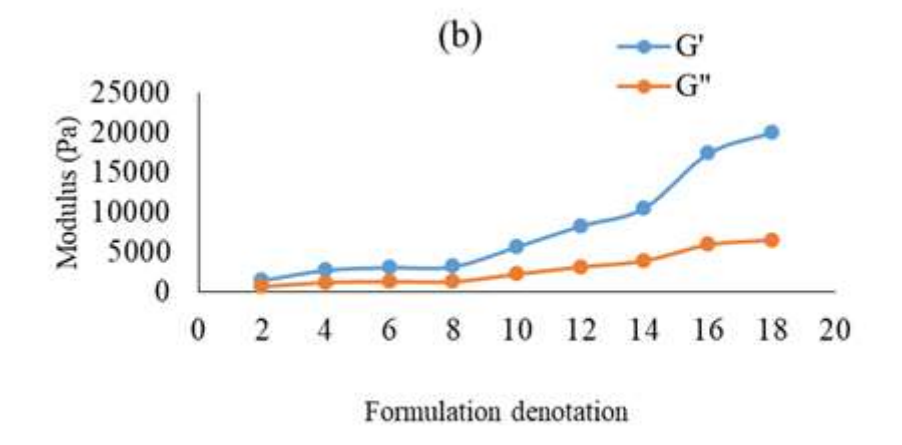


Fig. 3 G' and G" at 1 Hz for (a) xanthan gum added and (b) corn flour added formulation

xanthan gum) at 0.28±0.015 (Table 4). SIF was significantly (p<0.05) higher for corn flour-based formulations indicating their irregular cuboid shape and uneven edge surface area. Gholamipour et al. (2019) performed cold extrusion 3D printing of different hydrocolloid pastes and concluded formulations having SIF less than 60 could be considered as printable. Similarly, Lipton et al. (2015) calculated shape inconsistency index for 3D printed cookies and concluded that shape stability was decreased with increased fat content in food-inks.

Deformation factor

Deformation factor is an indicator of variation in surface area of upper edge and lower edge of symmetric cuboid shaped 3D food construct. Deformation factor was between 0.978 to 0.998 for xanthan gum added formulations whereas it was significantly (p<0.05) lesser for corn flour added formulations i.e., 0.92 to 0.97 as shown in Table 4. Gholamipour et al. (2019) suggested food inks having deformation factor more than 0.4 will be printable through extrusion-based printer.

Extrusion rate

Extrusion rate is calculated by dividing the weight of 3D printed construct with printing time and indicates about the extrudability of food inks. Softer food inks show high extrusion rate as compared to stiff and harder food inks at same extruding pressure. Extrusion rate was found to be highest at 2.5 g/min for F2 formulation and lowest at 1.63 g/min for F17. Except for F15 and F17 that showed no significant difference in extrusion rate, for all other formulations added with xanthan gum exhibited significantly (p<0.05) lower extrusion rate as compared to corn flour containing samples. It can be explained by the lower hardness values (data not presented) of formulations having corn flour as rheology modifier.

Correlation between viscoelastic characteristics and extrusion rate of the food inks

All the food inks were characterized as viscoelastic semi-solids with storage modulus (G') dominating over loss modulus (G") and phase angle was less than 25°. Also, all the formulations required certain yield stress before initiation of their flow under applied external stress. A strong negative correlation existed between extrusion rate and yield stress was observed for both xanthan gum added and corn flour added formulations and combined Pearson correlation coefficient was -0.717. It was found that with increase in total solid content of xanthan added formulations from F1 (50.25%) to F17 (61.77%), yield stress increased simultaneously from F1 (749 Pa) to F17 (2880 Pa) which rendered the formulations hard to extrude through the printing nozzle as evident by decrease in extrusion rate from F1 (1.96 g/min) to F17 (1.63 g/min).

Similarly, a strong positive correlation was observed between extrusion rate and phase angle for both xanthan gum and corn flour added formulations and combined Pearson correlation coefficient was 0.961. It can be inferred that phase angle was decreasing with increasing total solid contents of formulations, indicating that formulations were attaining more solid than viscous nature, which resulted in hard formulations requiring very high amount of external force to extrude and hence gradual drop-in extrusion rate was observed.

Conclusions

Apparent viscosity, yield stress and storage modulus of the formulations were critical for 3D printing of sweetened heat desiccated concentrated milk based dairy formulations incorporating XG and CF. The printability and strength depended on the rheology and composition of the formulations. Xanthan gum as RM imparted superior print quality as compared to those obtained from corn flour added formulations due to the pronounced shear thinning behaviour exhibited by them. Formulation prepared using milk concentrate to 45% TS, added with 30% sugar and 0.5% xanthan gum exhibited highest DAF (97.01%) and found to be best suited for 3D printing. Rheological characteristics viz., yield stress and phase angle are strongly correlated with the extrusion rate of the formulations keeping printing parameters constant and thus, printability of food inks can be predicted in advance by examining their rheological and textural attributes. Insights achieved from the investigation will aid in development of dairy sweetmeats with tailored structural, textural attributes using extrusion-based 3D food printing.

Acknowledgements

The authors gratefully acknowledge the Indian Council of Agricultural Research (ICAR), New Delhi for providing financial assistance.

References

Bareen MA, Joshi S, Sahu J K, Prakash S, Bhandari B (2021) Assessment of 3D printability of heat acid coagulated milk semi-solids 'soft cheese' by correlating rheological, microstructural, and textural properties. J of Food Eng 300: 110506

Choudhury DB., Kumari S, Hazarika M K (2024). 3D printed sweets made with peanut chenna and milk: A new frontier in food technology. J Food Process Eng 47. https://doi.org/10.1111/jfpe.14528

Dick A, Bhandari B, Prakash S (2019) 3D printing of meat. Meat Sci 153: 35-44

Gholamipour SA, Norton IT and Mills T (2019) Designing hydrocolloid based food-ink formulations for extrusion 3D printing. Food Hydrocolloids 95: 161-167

Gnezdilova AI, Burmagina TY, Kurenkova LA (2015) Investigation of rheological characteristics of concentrated milk products with a complex carbohydrate and protein composition Foods and Raw Mat 3: 60-64.

Joshi S, Sahu JK, Bareen MA, Prakash S, Bhandari B, Sharma N, Naik SN (2021) Assessment of 3D printability of composite dairy matrix by

- correlating with its rheological properties. Food Res Intl 141: 110111
- Lee CP, Karyappa R, Hashimoto M (2020) 3D printing of milk-based product. RSC Advances 10: 29821-29828
- Lille M, Nurmela A, Nordlund E, Metsä KS, Sozer N (2018) Applicability of protein and fiber rich food materials in extrusion based 3D printing. J Food Eng 220: 20-27
- Lipton JI, Cutler M, Nigl F, Cohen D, Lipson H (2015) Additive manufacturing for the food industry. Trends in Food Sci and Technol 43: 114-123
- Liu Y, Liu D, Wei G, Ma Y, Bhandari B, Zhou P (2018) 3D printed milk protein food simulant: Improving the printing performance of milk protein concentration by incorporating whey protein isolate. Innovative Food Sci and Emerging Technol 49: 116-126
- Paxton N, Smolan W, Böck T, Melchels F, Groll J, Jungst T (2017) Proposal to assess printability of bioinks for extrusion-based bioprinting and evaluation of rheological properties governing bioprintability. Biofabrication 9: 044107
- Sharma M, Parihar P, Dubey AD., Shukla SS, Soni, R., (2024). Additive manufacturing in the food industry: Innovations in customised fabrication and personalised nutrition. Food and Humanity 3, 100402. https://doi.org/10.1016/j.foohum.2024.100402

- Stokes JR, Frith WJ (2008) Rheology of gelling and yielding soft matter systems. Soft Matter 4: 1133-1140
- Suzuki Y, Takagishi K, Umezu S (2019) Development of a high precision viscous chocolate printer utilizing electrostatic inkjet printing. J Food Process Engg 42: e12934
- Zhao L, Pan F, Mehmood A, Zhang YH, Rehman AU, Wang Y (2020) Protective effect and mechanism of action of xanthan gum on the color stability of black rice anthocyanins in model beverage systems. Int J Bio Macromolecules 164: 3800-3807